Bosonic Spectral Density of Epitaxial Thin-Film La$_{1.83}$Sr$_{0.17}$CuO$_4$ Superconductors from Infrared Conductivity Measurements

J. Hwang,[1,*] E. Schachinger,[2] J. P. Carbotte,[1,3] F. Gao,[4] D. B. Tanner,[4] and T. Timusk[1,3]

[1]*Department of Physics and Astronomy, McMaster University, Hamilton, Ontario L8S 4M1Canada*
[2]*Institute of Theoretical and Computational Physics, Graz University of Technology, A-8010 Graz, Austria*
[3]*The Canadian Institute for Advanced Research, Toronto, Ontario M5G 1Z8, Canada*
[4]*Department of Physics University of Florida, Gainesville, Florida 32611, USA*

We use optical spectroscopy to investigate the excitations responsible for the structure in the optical self-energy of thin epitaxial films of La$_{1.83}$Sr$_{0.17}$CuO$_4$. Using Eliashberg's formalism to invert the optical spectra we extract the electron-boson spectral function and find that at low temperature it has a two component structure closely matching the spin excitation spectrum recently measured by magnetic neutron scattering. We contrast the temperature evolution of the spectral density and the two-peak behavior in La$_{2-x}$Sr$_x$CuO$_4$ with another high temperature superconductor Bi$_2$Sr$_2$CaCu$_2$O$_{8+\delta}$. The bosonic spectral functions of the two materials account for the low T_c of LSCO as compared to Bi-2212.

Despite 20 years of extensive research on the high critical temperature superconducting cuprates, there is as yet no consensus on the pairing mechanism or why T_c is so high. It is not known, for example, why most of the cuprate materials have a high T_c of over 90 K while another group, for example La$_{2-x}$Sr$_x$CuO$_4$ (LSCO), has a much lower T_c of about 30 K. Many theoretical ideas have been put forward such as the spin-charge separation [1], preformed pairs [2], exchange of spin fluctuations [3–9], and phonons [10–12] to list a few of the more prominent proposals. It took more than 45 years after the discovery of superconductivity in Hg before BCS theory was formulated. Yet less than ten years later, accurate and detailed measurements of the electron-phonon spectral density $\alpha^2F(\omega)$ responsible for the pairing were available from tunneling experiments for many of the conventional materials. This critical function followed from a numerical inversion, centered on the Eliashberg equations, of the current voltage characteristics of tunnel junctions [13]. Subsequently, optics was also used successfully to get comparable data [14,15] and $\alpha^2F(\omega)$ was calculated from first principles and used to calculate material specific superconducting properties which are often quite distinct from the universal laws of the BCS theory [16].

Many attempts have been made to obtain equivalent information in the cuprates. An important issue in such work is whether or not the idea of boson exchange mechanism and Eliashberg theory can in fact be used in highly correlated systems. Tunneling [6,12], angle-resolved photoemission [11,17,18], and optics [19–25] have all been used to determine an electron-boson spectral density in the oxide superconductors but with mixed results. Some argue that the resulting spectrum is characteristic of spin fluctuations while others attribute it to phonons. Accurate inelastic neutron scattering measurements of the bosonic spectra of both phonons and spin fluctuations followed by high

resolution optical or tunneling spectroscopy on the same material would go a long way towards settling this issue [26]. A related technique, angle-resolved photoemission (ARPES), is momentum resolved and has shown that the boson structure can depend on momentum [27]. Thus any definitive comparison with optics would require an average of the ARPES data taken at all momenta.

Very recently inelastic neutron scattering data on the local, i.e., momentum averaged spin susceptibility in LSCO have become available [28] and show two distinct energy scales. One peak is centered around 18 meV and the another near 40–70 meV with small features extending to 150 meV. In this Letter we invert data [29] on the optical conductivity of La$_{1.83}$Sr$_{0.17}$CuO$_4$ within an Eliashberg formalism with a Kubo formula for the conductivity to obtain the electron-boson spectral density [24]. We find a remarkable similarity with the neutron data which constitutes strong evidence for the spin fluctuation mechanism. We also compare our new results with previous results for Bi$_2$Sr$_2$CaCu$_2$O$_{8+\delta}$ (Bi-2212).

For optical spectroscopy La$_{2-x}$Sr$_x$CuO$_4$ material presents special problems because of the presence of c-axis longitudinal phonons in ab-plane optical spectra possibly mixed in by an unknown lattice defect. These effects are seen in most single crystal spectra [30]. Fortunately, in epitaxial films, these defects seem to be completely absent. We have therefore used the low noise data from Gao *et al.* for our reflectance data [29]. The films are 820 nm thick, grown on SrTiO$_3$ substrate by magnetron sputtering. The films show a superconducting transition at 31 K with a transition width of 1.5 K. The details of the measurements are given in Ref. [29]. The raw $\sigma(\omega)$ data for La$_{1.83}$Sr$_{0.17}$CuO$_4$ [29] show direct absorption by transverse optical phonons as well as the electronic background of interest here. After an appropriate subtraction of the phonons, the real and imaginary parts of the temperature

(T) and frequency (ω) dependent electronic conductivity $\sigma(T, \omega)$ are obtained. For correlated electrons, a generalized Drude form applies which defines an optical self-energy $\Sigma^{op}(T, \omega)$ through the equation

$$\sigma(T, \omega) = \frac{i\Omega_p^2}{4\pi} \frac{1}{\omega - 2\Sigma^{op}(T, \omega)}, \quad (1)$$

where Ω_p is the plasma frequency. The optical scattering rate $1/\tau^{op}(T, \omega)$ and the optical mass are related to $\Sigma^{op}(T, \omega)$ by $1/\tau^{op}(T, \omega) = -2\Sigma_2^{op}(T, \omega)$ and $\omega[m^{*op}(T, \omega)/m - 1] = -2\Sigma_1^{op}(T, \omega)$ where 1 and 2 denote real and imaginary parts.

Our method for determining the bosonic spectral density begins with the application of the maximum entropy inversion [24] of a simplified convolution integral which relates the measured scattering rate $1/\tau^{op}(T, \omega)$ to the electron-boson spectral density known to be remarkably accurate in the normal state. This gives a first numerical model for $I^2\chi(\omega)$ which we then further refine [25] through a least squares fit to the optical scattering rates using the full solutions of the Eliashberg equations and associated Kubo formula. This gives our final model. Details about the maximum entropy inversion and the d-wave Eliashberg equations can be found in Refs. [23,24].

In the top panel of Fig. 1 we present results for $1/\tau^{op}(T, \omega)$ versus ω for five temperatures. All data are in the normal state except for the last one (30 K) which is just below 31 K, the superconducting T_c of this film. The heavy curves correspond to the data which are used as the input in the inversion process. Our final results for the electron-boson spectral density $I^2\chi(\omega)$ are shown in the middle panel. Note the strong temperature dependence of the low energy structure. When this $I^2\chi(\omega)$ function is used in the Eliashberg equations, the optical scattering rates that result are shown in the top panel as the light lines. In all cases the fit to the data is good. For the 30 K data in the superconducting state d-wave symmetry was assumed for the gap channel.

The middle frame of Fig. 1 shows the extracted bosonic spectral density. Note that at 30 and 50 K both spectra show a two-peak structure with peaks at 15 and 44 meV. As the temperature is increased the spectral density evolves towards a single peak which broadens and moves to higher energies. We also note tails extending beyond 100 meV, but these have a low amplitude as compared to the peaks. All these features are in agreement with the data on the local spin susceptibility (shown in the inset) measured by polarized neutron scattering in a closely related sample by Vignolle *et al.* [28]. The data at 12 K show the same two-peak structure as we have found at 30 K. While Vignolle *et al.* have limited data at 300 K, they are also in accord with the temperature dependence of our spectra: the low energy peak in $I^2\chi(\omega)$, which exists only at low temperature, is absent above 100 K as it is in the neutron spectra at 300 K. The detailed agreement between $I^2\chi(\omega)$
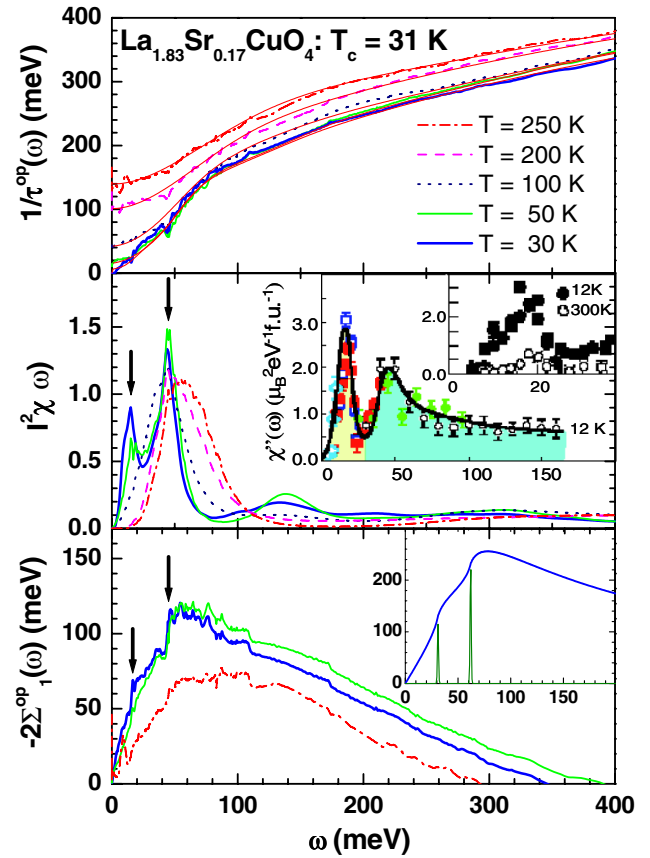

FIG. 1 (color online). Top panel: The optical scattering rate $1/\tau^{op}(\omega)$ in meV as a function of ω (in meV) for five temperatures. The heavy lines are the experimental data (TO phonons have been subtracted to isolate the electronic contribution). The light solid lines are the fits to the data. Middle panel: The electron-boson spectral density $I^2\chi(\omega)$ obtained from our Eliashberg inversion from the data in the top panel. The inset shows the data of Vignolle *et al.* for a closely related sample of $La_{2-x}Sr_xCuO_4$ with $x = 0.16$ and $T_c = 38.5$ K. In the inset of the inset the data with solid points are at 12 K and a comparison with 300 K data below 40 meV is also given (open points). Bottom panel: The real part of the optical self-energy $\Sigma_1^{op}(T, \omega)$ for LSCO. The arrows show the positions of the sharp peaks found in the spectral density at low temperature, $\omega = 15$ and $\omega = 44$ meV. Note the sharp rise in the self-energy at these frequencies. In the inset we show a simulated self-energy using a mode with two Einstein modes.

and the neutron data on the local magnetic susceptibility $\chi''(\omega)$ is strong evidence that the charge carriers in $La_{1.83}Sr_{0.17}CuO_4$ are coupled through a spin fluctuation mechanism. In related ARPES work on highly underdoped LSCO, Zhou *et al.* [11] interpret their results in terms of phonons. We note that the magnetic resonance peak is known to be very weak in highly underdoped materials [31] and that (as discussed above) nodal direction ARPES cannot be directly compared with momentum averaged optics.

A phenomenological model for the oxides where spin fluctuations replace the usual phonon exchange is the nearly antiferromagnetic Fermi liquid model (NAFFL) [3]. This model is well developed and is anchored in the generalized Eliashberg equations. While our approach to the inversion of the optical data might not apply in some highly correlated metals, it is fully justified in the NAFFL model. In particular, for a discussion of the applicability of Migdal's theorem (a precondition in our approach) we refer the reader to the review by Chubukov *et al.* [3].

Two-peak structure in the fluctuation spectrum of $La_{1.83}Sr_{0.17}CuO_4$ at low temperature and the disappearance of the lower peak at high temperatures can be seen directly in the optical self-energy itself which follows from the raw data without any appeal to microscopic models. This can be seen clearly in the bottom panel of Fig. 1 where we show our data for $-2\Sigma_1^{op}(T, \omega)$ for three temperatures, $T = 30$ K in the superconducting state (just below $T_c = 31$ K), at 50 K, above T_c, and 250 K. The heavy black arrows indicate the position of the two peaks in $I^2\chi(\omega)$. They coincide with sharp rises in $-2\Sigma_1^{op}(T, \omega)$. Such sharp rises are expected in the normal state for coupling of electrons to two Einstein oscillators as shown for a model calculation in the inset where a model spectrum $I^2\chi(\omega)$ has two peaks at 31 and 62 meV of width 1.2 meV with the second peak having twice the spectral weight of the first. The two peaks in $I^2\chi(\omega)$ can also be seen directly in the second derivative $2\pi W(\omega) = d^2[\omega/\tau^{op}(\omega)]/d\omega^2$ (not shown here) which is a model independent method and is known to be closely related to the spectral density in the peak region [15]. The red dash-dotted curve at $T = 250$ K shows a single rise consistent with a single peak in $I^2\chi(\omega)$ at this temperature.

It is interesting to compare LSCO with similar results for optimally doped Bi-2212 [25] ($T_c = 96$ K). These Bi-2212 data are shown in Fig. 2. The optical scattering rates on which our inversions are based are shown in the top panel while the lower panel shows our results for the spectral densities $I^2\chi(\omega)$. Only two temperatures are shown: 72 and 300 K for Bi-2212 (dashed curves) and 30 and 250 K for LSCO (solid curves). The scattering rates are very different in the two materials. The dashed curve for Bi-2212 shows a very steep rise with the midpoint at 92 meV which corresponds to the energy as the peak in the real part of the optical self-energy. By contrast the rise in the thick solid blue curve for LSCO is more gradual and proceeds on a broader energy scale. The rise starts close to zero energy because of the low energy peak in $I^2\chi(\omega)$ (thick solid blue curve in the bottom panel) and is much broader in energy because of the second peak around 50 meV. At higher temperatures the thin solid curve and the thin dashed red curve still show distinct variations with ω. For Bi-2122 the underlying spectrum $I^2\chi(\omega)$ has evolved to a single broad peak at about 100 meV plus a background. For LSCO the spectrum shows a sharper peak at about 55 meV and the
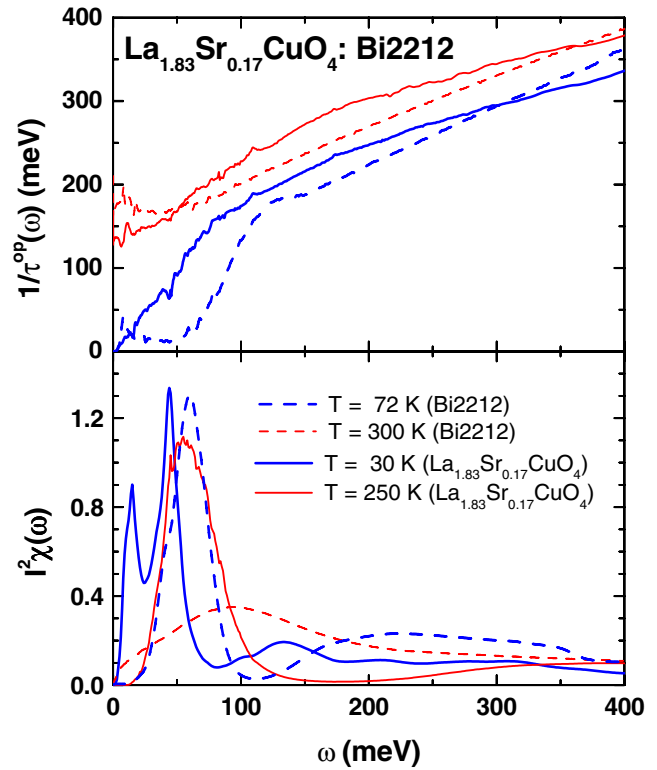

FIG. 2 (color online).   Top panel: Scattering rates for Bi-2212 (dashed lines) and LSCO (solid lines). The two materials show striking differences at low energies. Scattering sets in at very low energies in the LSCO material whereas Bi-2212 has a negligible scattering below 50 meV. Bottom panel: The bosonic spectral function $I^2\chi(\omega)$ of the same materials shown in the top panel. At low temperature LSCO has two peaks while Bi-2212 shows a single peak at much higher energy. As the temperature is raised the Bi-2212 peak is weakened dramatically and moves to high frequency [25] whereas in LSCO the lower peak vanishes while the upper peak remains up to 250 K. This difference at high temperature can already be seen in the top panel: the LSCO sample shows an onset of scattering in the 50 meV region while the Bi-2212 curve is quite featureless at 300 K.

background in comparison is small. This translates into a room temperature scattering rate in Bi-2212 which is featureless and flat while in LSCO the bosonic peak is very much present giving rise to a marked shoulder in the scattering rate in the 50 meV region.

What are the implications of these spectra for superconductivity? T_c in Bi-2212 is 3 times larger than in LSCO. For an *s*-wave electron-phonon superconductor the same spectral density $I^2\chi(\omega)$ enters both renormalization and gap channels of the Eliashberg equations. In a *d*-wave superconductor, however, the spectral density that enters the gap channel is a *d*-wave projection of the electron-boson exchange process rather than its *s*-wave projection which we have determined from optics and shown in the middle panel of Fig. 1 and the lower panel of Fig. 2. For simplicity we can assume that these two quantities differ

mainly by a numerical factor [32]. This factor can be fit to the known value of the critical temperature T_c which we determine from the complete numerical solutions of the d-wave Eliashberg equations. We find that T_c is well represented by the simple modification of the McMillan equation [33,34]

$$k_B T_c \cong \hbar \omega_{ln} \exp\left[-\frac{1 + \lambda^s}{\lambda^d} \right], \qquad (2)$$

where $1 + \lambda^s$ comes from the normal state renormalization of the dispersion curves and λ^d is the interaction in the gap channel. Here ω_{ln} is the average boson energy defined by Allen and Dynes [35] and is the same for s- or d-channel cases.

Using our $I^2\chi(\omega)$ functions we find that the λ^d values are nearly the same for Bi-2212 (1.85) and LSCO (1.90). However the value of ω_{ln} differ by a factor of 2, ~50 meV for Bi-2212 and ~25 meV for LSCO. Therefore the softening of the spin fluctuation spectrum in LSCO as compared to Bi-2212 accounts for a factor of 2 difference in T_c. The remaining difference is traced to the value of λ^s which is larger in LSCO (3.40) as compared to Bi-2212 (2.50). The renormalization factor $1 + \lambda^s$ in the modified McMillan equation [Eq. (2)] is pair breaking and this accounts for the rest of the difference in T_c values. While we do not predict T_c we can explain in a robust way from our analysis the factor of 3 difference in T_c between LSCO and Bi-2212 samples.

In summary, we have measured the fluctuation spectrum in LSCO $I^2\chi(\omega)$ at various temperatures. At low temperature it shows two characteristic energy scales in remarkable agreement with the local (q averaged) spin susceptibility recently found in polarized inelastic neutron scattering experiments. As the temperature is increased, the low energy peak disappears in accord with the neutron results. While the maximum entropy technique and least squares fit to the measured optical scattering rates within an Eliashberg framework are employed here, the two-peak structure in $I^2\chi(\omega)$ can be seen directly in the raw data for the real part of the optical self-energy. In contrast optimally doped Bi-2212 reveals a very different behavior showing a single sharp peak centered at 60 meV with a valley above it and a broad low intensity background extending to energies up to 400 meV. Finally, the bosonic spectra derived from our analysis fully account for the low superconducting transition temperature of LSCO as compared to Bi-2212.

*hwangjs@mcmaster.ca
[1] P. W. Anderson, *The Theory of Superconductivity in the High-T_c Cuprates* (Princeton University, Princeton, NJ, 1997).
[2] V. J. Emery and S. A. Kivelson, Nature (London) **374**, 434 (1995).
[3] A. V. Chubukov *et al.*, in *The Physics of Conventional and Unconventional Superconductors*, edited by K. H. Bennemann and J. B. Ketterson (Springer-Verlag, Berlin, 2003).
[4] J. P. Carbotte, E. Schachinger, and D. N. Basov, Nature (London) **401**, 354 (1999).
[5] Ar. Abanov and A. V. Chubukov, Phys. Rev. Lett. **83**, 1652 (1999).
[6] J. F. Zasadzinski *et al.*, Phys. Rev. Lett. **96**, 017004 (2006).
[7] J. C. Campuzano *et al.*, Phys. Rev. Lett. **83**, 3709 (1999).
[8] M. R. Norman and H. Ding, Phys. Rev. B **57**, R11089 (1998).
[9] P. D. Johnson *et al.*, Phys. Rev. Lett. **87**, 177007 (2001).
[10] A. Lanzara *et al.*, Nature (London) **412**, 510 (2001).
[11] X. J. Zhou *et al.*, Phys. Rev. Lett. **95**, 117001 (2005).
[12] J. Lee *et al.*, Nature (London) **442**, 546 (2006).
[13] W. L. McMillan and J. M. Rowell, Phys. Rev. Lett. **14**, 108 (1965).
[14] B. Farnworth and T. Timusk, Phys. Rev. B **10**, 2799 (1974).
[15] F. Marsiglio, T. Startseva, and J. P. Carbotte, Phys. Lett. A **245**, 172 (1998).
[16] J. P. Carbotte, Rev. Mod. Phys. **62**, 1027 (1990).
[17] A. A. Kordyuk *et al.*, Phys. Rev. Lett. **97**, 017002 (2006).
[18] T. Valla *et al.*, Phys. Rev. Lett. **98**, 167003 (2007).
[19] R. T. Collins *et al.*, Phys. Rev. B **39**, 6571 (1989).
[20] A. V. Puchkov, D. N. Basov, and T. Timusk, J. Phys. Condens. Matter **8**, 10049 (1996).
[21] J. J. Tu *et al.*, Phys. Rev. B **66**, 144514 (2002).
[22] S. V. Dordevic *et al.*, Phys. Rev. B **71**, 104529 (2005).
[23] J. P. Carbotte and E. Schachinger, Ann. Phys. (Leipzig) **15**, 585 (2006).
[24] E. Schachinger, D. Neuber, and J. P. Carbotte, Phys. Rev. B **73**, 184507 (2006).
[25] J. Hwang, T. Timusk, E. Schachinger, and J. P. Carbotte, Phys. Rev. B **75**, 144508 (2007).
[26] M. Chiao, Nature Phys. **3**, 148 (2007).
[27] T. Sato *et al.*, J. Phys. Soc. Jpn. **76**, 103707 (2007).
[28] B. Vignolle *et al.*, Nature Phys. **3**, 163 (2007).
[29] F. Gao *et al.*, Phys. Rev. B **47**, 1036 (1993).
[30] M. Reedyk and T. Timusk, Phys. Rev. Lett. **69**, 2705 (1992).
[31] Z. Yamani *et al.*, Physica (Amsterdam) **460–462C**, 430 (2007)
[32] J. P. Carbotte and E. Schachinger, *Model and Methods of High-T_c Superconductivity*, edited by J. K. Srivastava and S. M. Rao (Nova Science, Hauppauge, NY, 2003), p. 73.
[33] W. L. McMillan, Phys. Rev. **167**, 331 (1968).
[34] P. J. Williams and J. P. Carbotte, Phys. Rev. B **39**, 2180 (1989).
[35] P. B. Allen and R. C. Dynes, Phys. Rev. B **12**, 905 (1975).